^{27}Al nuclear magnetic resonance detection of diffusion processes in $Ni_{1-x}Al_x$ $(0.46 \leqslant x \leqslant 0.54)$ and Ni_2Al_3

1997 J. Phys.: Condens. Matter 9 6085

(http://iopscience.iop.org/0953-8984/9/28/007)

J. Phys.: Condens. Matter **9** (1997) 6085–6095. Printed in the UK PII: S0953-8984(97)81689-X

^{27}Al nuclear magnetic resonance detection of diffusion processes in $Ni_{1-x}Al_x$ ($0.46 \leqslant x \leqslant 0.54$) and Ni_2Al_3

T J Bastow†§, M E Smith†‡ and G W West†

† CSIRO Division of Materials Science and Technology, Private Bag 33, South Clayton MDC, Clayton, Victoria 3169, Australia

‡ Department of Physics, University of Kent, Canterbury, Kent CT2 7NR, UK

Received 7 February 1997

Abstract. The alloy system $Ni_{1-x}Al_x$ has been investigated by means of ^{27}Al NMR around the equiatomic region where $x = 0.5$, and at $x = 0.6$, which gives the trigonal ordered compound Ni_2Al_3. For Ni_2Al_3, two Al sites were clearly resolved at room temperature by means of their characteristic second-order quadrupolar structure. NMR spectra for cubic $Ni_{1-x}Al_x$ taken at temperatures up to 960 °C show rapid ^{27}Al line narrowing above $\simeq$600 °C for $x = 0.54$ (indicative of diffusion processes), but no such line narrowing was observed up to 960 °C for $x = 0.50$ or $x = 0.48$. ^{61}Ni NMR results are also reported for the equiatomic alloy. For Ni_2Al_3, the ^{27}Al NMR powder pattern evolved smoothly into that characteristic of one well defined site as the temperature was raised to 820 °C, although no phase transition was detected by means of powder x-ray diffraction or thermal analysis. These observations are discussed qualitatively in terms of defect-assisted diffusion processes.

1. Introduction

Nickel–aluminium alloys have attracted much technological interest because of their possible high-temperature structural applications in hostile environments [1, 2]. Most practical applications so far have made use of the superalloy Ni_3Al [3], but alloys with other compositions, like equiatomic NiAl, are also of interest [4]. NiAl has already been used as a high-temperature oxidation-resistant coating [5]; its density being lower than that of nickel-based superalloys makes it potentially attractive for aerospace applications [6]. Many of the high-temperature properties are related to atomic-scale motions, and achieving an improved understanding of the structure–dynamics relationship is of substantial interest. The present work uses ^{27}Al NMR as a probe of the local structure in some Al-rich NiAl alloys (providing information complementary to that already obtained from x-ray diffraction (XRD) and electron diffraction investigations), and of the influence of varying stoichiometry (i.e. vacancy concentration) on the diffusive atomic motion at elevated temperatures.

The total chemical shift range for ^{27}Al in insulating materials, namely oxides, nitrides, zeolites, etc, is useful but not large ($\simeq$100 ppm), and techniques such as magic-angle spinning are necessary to provide sufficient spectral resolution [7]. However, in metals, the effect of the contact interaction between the conduction electrons and the nuclei, combined with the Pauli paramagnetic susceptibility, leads to an enhanced shift (termed the Knight shift [8]), which is typically one to two orders of magnitude larger than the chemical shift

§ Author to whom any correspondence should be addressed.

0953-8984/97/286085+11$19.50

for insulators. Although the linewidths may be large, the Knight shift range is also large, and often permits the resolution of distinct atomic sites in the specimen. The use of NMR as a microscopic probe for metals and alloys originated with work of Knight and Bloembergen and their co-workers in the early 1950s, and is summarized in the review by Drain [9] and in the book by Carter *et al* [10]. The case of dilute alloys of aluminium in magnesium provides a recent example where such metallic shifts permitted discrimination between aluminium in solid solution in magnesium and aluminium in the $Mg_{17}Al_{12}$ precipitate phase [11]. Furthermore, they enabled the three distinct magnesium sites in the $Mg_{17}Al_{12}$ unit cell to be clearly resolved by means of ^{25}Mg NMR.

Previous NMR data exist for NiAl alloys, with the first detailed study being that by West in 1964, where a Knight shift of 630 ± 30 ppm was reported [12]. The main conclusions from this early work were that the Knight shift was, to within the accuracy of the measurements, independent of composition, and that, even far from the 1:1 stoichiometry, the aluminium linewidth remained quite constant. Subsequent studies have remeasured the line-shift and linewidth as functions of the composition [13–15]. An extensive study by Rubini *et al* looked in detail at the martensitic transformation for the β-phase using ^{27}Al NMR for nickel-rich alloys [16, 17]. More recently, the effect of small additions of manganese on the properties of NiAl intermetallic compounds has been examined by means of ^{27}Al solid-state NMR [18]. However, the work cited in the previous NMR references was largely performed in electromagnets with applied fields B_0 of order 1 T (except the recent work by Rubini *et al*), where the ^{27}Al quadrupolar interactions reported below for Ni_2Al_3, and elsewhere for gamma phase TiAl [19], render the ^{27}Al resonance essentially unobservable. Since about 1970, the common use of pulsed NMR spectrometers in conjunction with high-field superconducting magnets has increased the detection sensitivity by several orders of magnitude, and decreased the second-order quadrupole broadening of the lines (which varies in Hz as B_0^{-1} [20]). The present study uses a higher magnetic field than earlier work, which narrows these large quadrupolar interactions, provides a more accurate measure of shift changes with composition, and enables the effects of changing temperature on the spectra to be detected.

Table 1. ^{27}Al NMR Knight shifts and linewidths (FWHM) for $Ni_{1-x}Al_x$ alloys.

Atomic percentage of Al	Linewidth $\Delta\nu$ (kHz)	Knight shift (ppm)
46	20.8	694
48	17.7	653
50.4	7.9	630
52	11.0	630
53	16.2	605
54	22.0	592

The work detailed below divides into two parts. The first is concerned with variations in stoichiometry about that of the equiatomic alloy NiAl, which has the CsCl structure. Six alloys $Ni_{1-x}Al_x$, with $x = 0.46$, 0.48, 0.50, 0.52, 0.53, and 0.54, were prepared, and their static wide-line ^{27}Al NMR spectra measured at room temperature. The original powder XRD work on these alloys [21] indicated that, within the β-phase field, for $x < 0.5$ (i.e. for nickel-rich alloys) there were nickel substitutions on the aluminium sublattice, while for $x > 0.5$ there were vacancies on the nickel sublattice. In the light of this observation it seemed reasonable to suppose that the existence of vacancies might facilitate atomic motion at temperatures well below T_m (=1635 °C for NiAl), so spectra were recorded up to 960 °C.

The only NMR-active nickel isotope, ^{61}Ni, has nuclear spin $I = 3/2$ (and therefore also a quadrupole moment), and a moderate gyromagnetic ratio, but is only 1.19% abundant. This paper reports a clear observation of ^{61}Ni NMR in a diamagnetic alloy. The second part of this work is concerned with structure and motion in the compound Ni_2Al_3 (with $x = 0.6$), which may be thought of as the logical limit of the $x > 0.5$ series, where the vacancies on the nickel sublattice have condensed, and a new ordered structure has formed. An explanation for the observed spectral changes in terms of diffusive motion is given.

2. Experimental details

2.1. Alloy preparation and characterization

Nickel and aluminium in suitable proportions were melted together (with subsequent remeltings) in an argon arc furnace, with a water-cooled copper hearth, until satisfactory homogeneity was achieved. The stoichiometry was carefully checked as previously reported in detail [12]. The powder for the NMR specimen was obtained by crushing the brittle ingot to a mesh size of $\simeq$200 μm. This was then heated at 1000 °C for two hours in argon to anneal out defects caused by crushing. This powder was then used, without further coating or particle separation, for NMR analysis. The XRD analysis was carried on a Siemens D500 diffractometer using Cu Kα radiation scanning at a rate of 1° (2θ) min^{-1} over a range of 30° to 70°. Experiments were carried out *in situ* up to 650 °C using an Anton Parr HTK hot-platinum-strip high-temperature stage. Thermal analysis was performed by differential scanning calorimetry on a Setaram instrument, for both heating and cooling of the sample.

2.2. NMR

Static ^{27}Al NMR spectra were obtained with a Bruker MSL 400 spectrometer using a superconducting magnet with a nominal field of 9.4 T, and operating at a frequency of 104.2 MHz. Frequency offsets of up to 2 MHz were used for observing the satellite transitions in Ni_2Al_3. For the room temperature spectra, a 4 mm magic-angle spinning (MAS) probe was used without sample rotation—purely for the convenience of having a small coil and consequently a small sample size, and the ability to accurately tune and match the probe. The ^{27}Al NMR linewidths in all of the specimens studied here were too large to be usefully narrowed by MAS. For work above room temperature, a water-cooled probe, with a resistance furnace heating both the specimen and the coil, designed in this laboratory, was used. This was capable of operating continuously at temperatures up to at least 960 °C. The probe used a five-turn transverse rf coil with an internal diameter of 7 mm. For the high-temperature measurements, the samples were sealed under vacuum in quartz capsules.

To observe the broad lines in these alloys, all of the spectra were obtained using an echo sequence, D1–t–D2–t–acq, with phase cycling using 16 steps [22], which efficiently cancelled any transmitter pulse breakthrough. To ensure a uniform power spectrum over the ^{27}Al lines encountered here, the sub-90° rf pulses D1 = 2 μs and D2 = 4 μs were used with an echo time (t) of 20 ms. Spectra were referenced to ^{27}Al in $Al(H_2O)_6^{3+}$ at zero ppm shift, via the ^{27}Al resonance from octahedrally coordinated aluminium, in $Y_3Al_5O_{12}$ at 0.7 ppm. The frequency axes for the spectra displayed here are graduated in either ppm (parts per million) or kHz (MHz) shift from this zero. ^{61}Ni static spectra were acquired using similar methods at a frequency of 35.75 MHz with a 4 mm probe. The Knight shift for ^{61}Ni was obtained by comparison with the Larmor frequency of ^{35}Cl in aqueous NaCl, and taking

the known magnetic moments [23] of ^{35}Cl (=0.8218743 μ_N (nuclear magnetons)) and ^{61}Ni (=−0.750 02 μ_N) to give the shift from a diamagnetic nickel environment.

3. Results and discussion

3.1. $Ni_{1-x}Al_x$

Six alloys, with $x = 0.46$, 0.48, 0.50, 0.52, 053, and 0.54, were initially examined, and the ^{27}Al NMR spectra gave a single symmetric Gaussian-shaped resonance. The ^{27}Al Knight shift of the equiatomic alloy is approximately 580 ppm, consistent with the values of ∼600 ppm previously reported (e.g. in [12, 16]). It has been argued [16] that as the change in the ^{27}Al shift is small at around $x = 0.50$ compared to the change in the density of states deduced from the specific heat (which is largely due to d electrons), the ^{27}Al shift must be dominated by s electrons. Compare the value of 580 ppm measured here for $Ni_{0.5}Al_{0.5}$ with the 1640 ppm shift for pure aluminium metal. This reduction of the shift in the alloy occurs mainly because of the reduced s-electron character at the Fermi surface [24]. In nickel-rich alloys, as nickel is added, there is a very small increase in the s susceptibility [16] that is manifested here as a small positive shift. On a finer scale here, there is the progressive decrease in Knight shift with increasing Al content that is simply a continuation of the trend observed for the nickel-rich alloys. The overall change in Knight shift, in going from $x = 0.46$ to $x = 0.54$, is 102 ppm (table 1), which simply continues the trend of decreasing s-electron density at the Fermi surface as aluminium is added. A low density of states at the Fermi surface is also consistent with our measured spin–lattice relaxation time of 92 ms for $Ni_{0.5}Al_{0.5}$.

NMR linewidth measurements as functions of temperature are capable of detecting diffusional motion of the nucleus (atom) observed, and in principle yielding estimates for the diffusion constant and activation energy for site hopping. An early observation of direct relevance here was for ^{27}Al in metallic aluminium by Seymour [25], where strong line narrowing set in above about 280 °C, well below the melting point at 660 °C, the ratio of these absolute temperatures being approximately 0.6. Since the melting point of equiatomic NiAl is 1635 °C, then using the same ratio (0.6), it would appear unreasonable to expect observation of appreciable diffusional motion at temperatures below 870 °C. However, since it is known that vacancies exist in $Ni_{1-x}Al_x$ for $x > 0.5$, which might assist diffusional motion, the ^{27}Al NMR spectrum of the alloy with $x = 0.54$ was measured at a series of temperatures up to 960 °C. Significant line narrowing was indeed observed above about 600 °C (figure 1). As a check, the spectra of the alloys $x = 0.48$, 0.50, and 0.53 were also monitored up to 960 °C (figure 1). Only a slow linear decrease in linewidth was observed for the $x = 0.48$ and 0.50 samples, consistent with thermal expansion of the lattice and the consequent progressive reduction in dipolar and defect-originating quadrupolar contributions. Note that the latter contributions should be absent from the stoichiometric $x = 0.5$ alloy, consistent with the considerably narrower line observed for it (table 1) compared to those for the alloys with stoichiometries away from 0.5. The line narrowing for the $x = 0.53$ alloy is intermediate between the line narrowings for $x = 0.48$ and $x = 0.50$ and that for the $x = 0.54$ sample, indicating the importance of defects in assisting the diffusional process. Here, detailed analysis to extract the diffusion constant and activation energy is not warranted, since for the analysis to be accurate the motionally narrowed limiting values of the curves in figure 1 are required, and these need temperatures well in excess of that of our current NMR probe. This information would be available from measurements

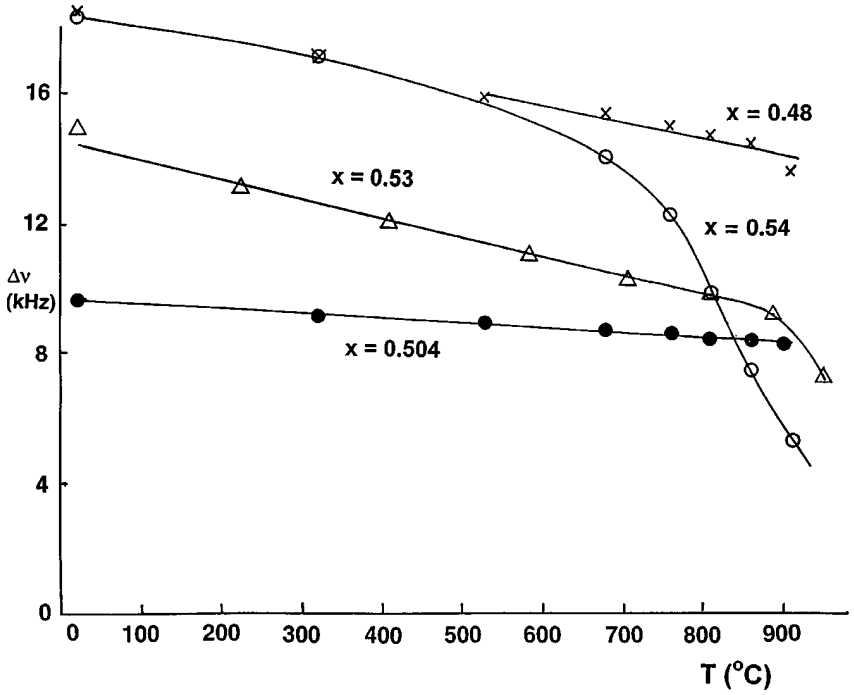

Figure 1. The linewidth (FWHM, $\Delta\nu$) of the ^{27}Al NMR line for cubic $Ni_{1-x}Al_x$ alloys as a function of temperature. The full lines are a guide to the eye.

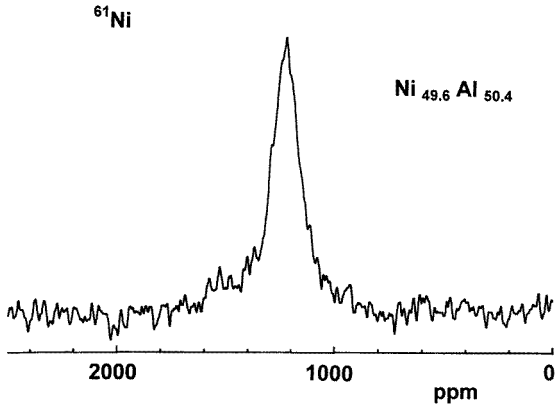

Figure 2. The ^{61}Ni NMR line-shape for equiatomic NiAl.

at higher temperatures, and is of some importance in tailoring the properties of such alloys.

The ^{61}Ni signal from an equiatomic alloy is shown in figure 2; it is a single resonance of linewidth 5.5 kHz at a shift of 1220 ppm from the diamagnetic nickel position. This is one of the few reports of a Knight shift for nickel, and can be compared with a previously reported value of 1890 ppm obtained for such an alloy [26]. The discrepancy between these results is not surprising given the difficulties of measurement at the lower field of 1.6 T of the

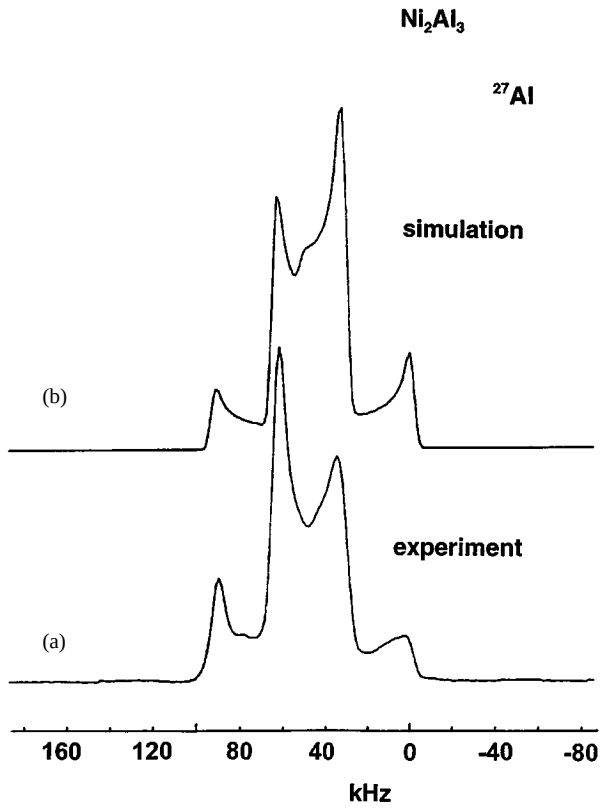

Figure 3. (a) The ^{27}Al NMR powder line-shape for the Al1 and Al2 site $(-1/2, 1/2)$ transitions in Ni_2Al_3 at room temperature, (b) the simulation of the line-shape, and (c) powder line-shapes of the first-order quadrupole satellite transitions for the two Al sites.

previous study [26] and the critical nature of the exact value of the magnetic moments used to calculate the diamagnetic position. However, the susceptibility measurements [12] and the relatively small positive Knight shifts determined here for ^{61}Ni and ^{27}Al are consistent with a view that the d band in such alloys is full.

Table 2. The ^{27}Al nuclear quadrupole coupling constants C_Q, C'_Q, and the Knight shift anisotropy (KSA) for the aluminium sites Al1 and Al2 in Ni_2Al_3. (For the definition of the symbols, see the text).

Site	C_Q (MHz)	C'_Q (MHz)	KSA (ppm)
Al1	16.37	17.8	81
Al2	9.67	10.9	41

3.2. Ni_2Al_3

The spectrum for this specimen (figure 3(a)) is most simply interpreted as a pair of overlapping second-order quadrupole spectra, each with $\eta = 0$, corresponding to two

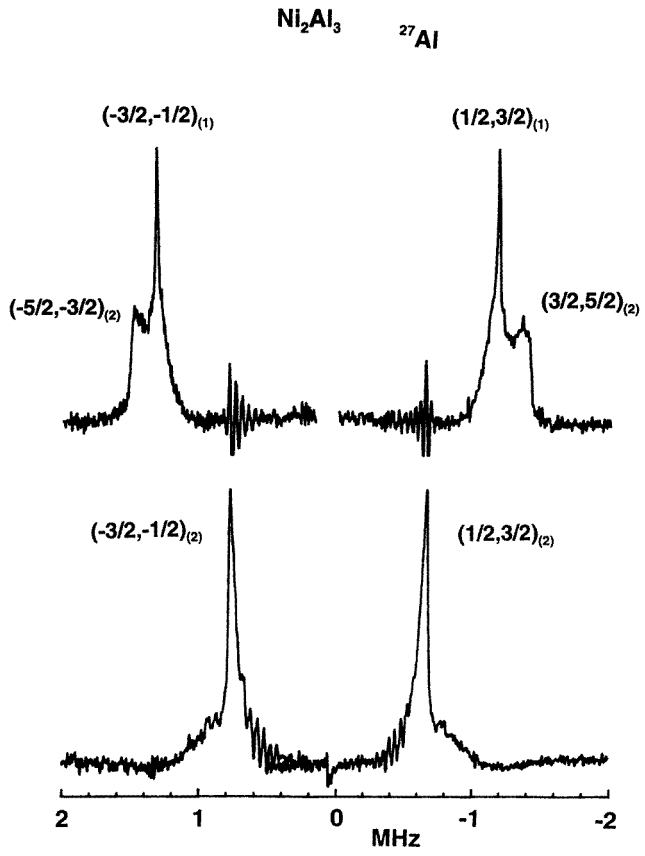

(c)

Figure 3. (Continued)

inequivalent Al sites in the unit cell. The simulation, using the Bruker program POWDER, shown in figure 3, indicates an integrated intensity ratio of approximately 1:2 with the line corresponding to the higher C_Q $(=e^2qQ/h)$ having the lower intensity. This agrees with the established x-ray structure [1], trigonal, with space group $P\bar{m}1$ (No 164), which has two inequivalent Al atoms in the unit cell: Al1 at site 1a with point symmetry $\bar{3}m$ and Al2 at site 2d with symmetry $3m$. Although the simulation in figure 3 gives results which are physically satisfactory, and clearly shows two sites with considerably different values of C_Q, the observed intensity ratios of the high- and low-frequency peaks for each spectrum are reversed with respect to the simulation. This suggests that there might exist here appreciable Knight shift anisotropy, neglected in a purely second-order quadrupole simulation (figure 3(b)), which is distorting the fit, optimized with respect to peak separation, to give an effective quadrupole coupling of C'_Q for each site of 17.8 and 10.9 MHz, with the integrated intensities being in the ratio 1:2. The first-order quadrupole satellite transitions for each site were therefore located, and a true value of C_Q determined for each site from the separation of the $(-3/2, -1/2)$ and $(1/2, 3/2)$ satellites: $(3/20)C_Q$. Some of the satellites are shown in figure 3(c); they give values for C_Q of 16.37 and 9.67 MHz respectively. Note that the C_Q-values from the satellite transitions are approximately an order of magnitude numerically more precise and appreciably lower (10–15%) than the values deduced from

the second-order spectrum assuming that only the quadrupole interaction contributes. By taking the positions of the singularities for the central transition [27] for an axially symmetric case (which is expected from the site symmetries), a quadratic equation in the Knight shift anisotropy K_{ax} can be written down and solved, knowing the estimated and real C_Q (written here as $\nu_Q = 3C_Q/20$ in equation (1)):

$$K_{ax} = 5\nu_Q[\pm\nu'_Q - \nu_Q]/\nu_L^2. \tag{1}$$

Solving this equation (taking the physically plausible positive sign) yields estimates of K_{ax} of 81 and 41 ppm for the Al1 and Al2 sites respectively. A similar value of K_{ax} is found for TiAl, where C_Q is of order 10 MHz at the aluminium site [19]. The NMR data for Ni_2Al_3 are collected together in table 2.

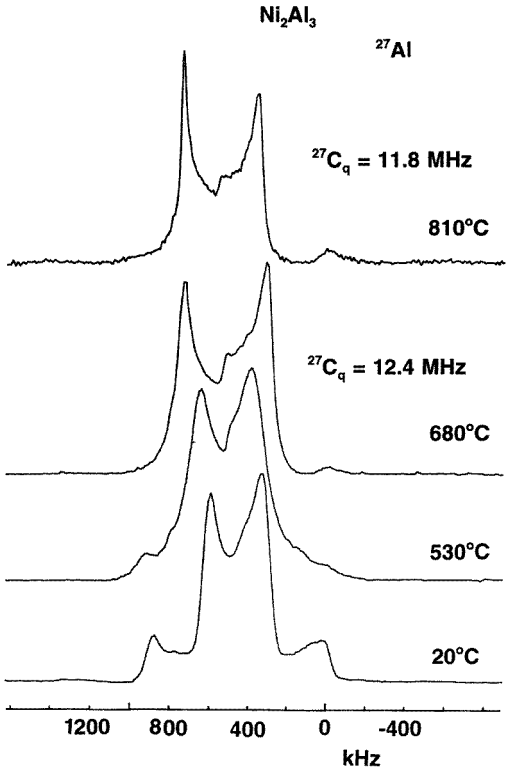

Figure 4. The temperature dependence of the $(-1/2, 1/2)$ powder line-shape in Ni_2Al_3.

Given the strong enabling effect of vacancies on aluminium diffusion in aluminium-rich NiAl, it was natural to enquire whether the condensed plane of vacancies in Ni_2Al_3 gave rise to enhanced diffusional behaviour at elevated temperatures. The ^{27}Al spectra of Ni_2Al_3 at a series of temperatures up to 820 °C are shown in figure 4. This illustrates what *appears* to be a gradual transformation from a spectrum characteristic of a two-site structure at room temperature to a spectrum, very sharply defined at 820 °C (more so than the room temperature line-shape), belonging to a different one-site structure. The spectrum is characteristic of a well defined quadrupolar interaction with the more sharply defined features presumably resulting from averaging of dipolar interactions. A parallel powder XRD examination showed no change in the x-ray line positions apart from small

changes consistent with thermal expansion, and differential scanning calorimetry revealed no structural transformation in the temperature range studied. The explanation for the change in the appearance of the spectrum would appear to be that rapid hopping has produced an averaging effect which leads to one effective C_Q.

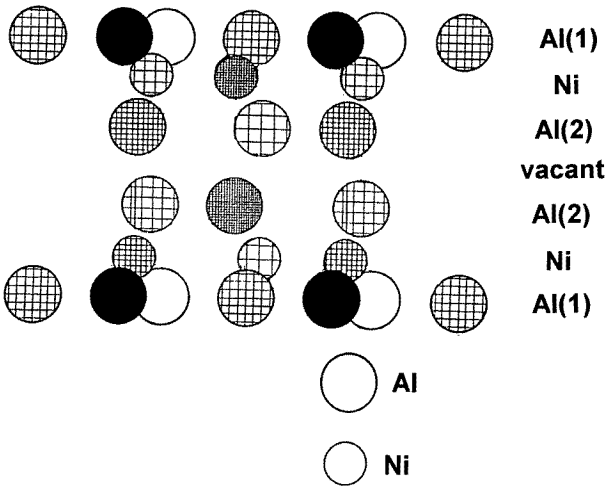

Figure 5. The stacking sequence of the Al(1), Al(2), and Ni planes in Ni_2Al_3, showing the vacant Ni plane into which, it is suggested, the Al atoms are excited, allowing an Al(1) $\leftrightarrow$ Al(2) interchange. The atoms are shaded to indicate depth; the nearest being the darkest. The vertical direction into the page is approximately the [111] direction of the precursor cubic β-phase. This figure was adapted from reference [21].

To explain the change in the ^{27}Al NMR spectrum, consider the following model of the Ni_2Al_3 system (closely resembling real Ni_2Al_3). The unit cell of the structure has two aluminium sites, Al1 (of population 1) and Al2 (of population 2). The ^{27}Al isotropic shifts of Al1 and Al2 are very similar, but their (second-order) quadrupolar interactions are different. It is assumed that $C_{Q1} > C_{Q2}$, and that the interactions are axial and collinear (as for real Ni_2Al_3). Assume that intersite hopping, namely Al1 $\leftrightarrow$ Al2, can take place if the crystal temperature is then raised. In real Ni_2Al_3 this can be done by first thermally exciting some aluminium atoms into the vacant Ni sheet (described by Bradley and Taylor [21] in their initial description of Ni_2Al_3 as trigonally distorted b.c.c.), which then allows an Al1 atom to hop to a vacant Al2 site and vice versa (see figure 5). Now consider a low-temperature ^{27}Al single-crystal rotation pattern, rotating from $\boldsymbol{c}$ parallel to $\boldsymbol{B}_0$ to $\boldsymbol{c}$ perpendicular to $\boldsymbol{B}_0$, for our model Ni_2Al_3. (The KSA is being neglected here as a first approximation.) The frequency spectrum at arbitrary angle is just two lines, one from each site, which move with the angle such that the second-order patterns that they trace out *are precisely in phase*; that is

$$\nu = (\nu_Q^2/2\nu_L)(\cos^2\theta - 1)(9\cos^2\theta - 1). \tag{2}$$

For a polycrystalline specimen at low temperatures, a spherical average over orientations gives, for each site, a powder pattern. When these two powder patterns are superimposed, the result looks like the experimentally observed pattern for real Ni_2Al_3. If there is rapid hopping, Al1 $\leftrightarrow$ Al2, then, for a single crystal at an arbitrary orientation θ, this will result in a single line at some average frequency ν_{av} which, for a first-order splitting, would be the weighted mean $(\nu_1 + 2\nu_2)/3$. However, the shifts here are second order. This will result in

a rotation pattern, in phase with the other two, so the resultant high-temperature powder pattern will be that for a single site with the quadrupole frequency

$$\nu_{Q,av} = (\nu_{1Q} + 2\nu_{2Q})/3.$$

The justification for this assertion is that with rapid hopping (estimated at this temperature to be occurring on a timescale of the order of nanoseconds) the two quadrupolar Hamiltonians (linear in ν_Q) will be averaged to a weighted mean before acting on the system. The average quadrupolar Hamiltonian then acts on the system on a timescale of the order of ms. The average value observed for C_Q is very close to the weighted average of the room temperature values of C_Q. As the temperature increases, the average value drifts down slightly (figure 4), consistently with small changes in the site distortions with thermal expansion. Note that, in general, most of the couplings C_Q decrease monotonically with temperature.

The motivation for invoking atomic Al jumping in the first place comes from the observations described above on thermally induced ^{27}Al line narrowing in β-phase $Ni_{1-x}Al_x$ ($0.5 < x < 0.55$). In this region there are nickel vacancies on the nickel sublattice. The limit $x = 0.55$ defines the phase boundary (at 20 °C). In the Al-rich β-phase, ^{27}Al line narrowing takes place at progressively lower temperatures as x is increased towards 0.55. We believe that the Ni_2Al_3 structure, which can be viewed as a trigonally distorted b.c.c. structure with every third Ni(111) plane missing, is the long-range-ordered end-point of the defect structure present locally for $0.50 < x < 0.55$, a view which is consistent with the motion observed.

4. Conclusion

Substantial atomic motion can be detected by means of ^{27}Al NMR in Al-rich NiAl alloys at temperatures well below the melting point. For the ordered alloy Ni_2Al_3, the ^{27}Al spectrum reveals details of the crystal structure through the large difference between the nuclear quadrupole couplings (C_Q) at the two Al sites. For Ni_2Al_3, above $\simeq$600 °C, the motion occurs rapidly on the NMR timescale, producing a spectrum characteristic of a single averaged C_Q. The ease of motion in these aluminium-rich alloys seems to be strongly related to the presence of constitutional vacancies.

Acknowledgments

The authors are grateful to Dr D G Hay for XRD measurements, Dr M Forsyth for the loan of a probe, Dr C Bessada for thermal analysis, Dr M Gibson for some of the alloy preparations, Darryl Jones for specimen encapsulation, and Stephen Stuart for useful discussions.

References

[1] Baker I, Darolia R, Whittenberger J D and Yoon M H (ed) 1993 *High-Temperature Ordered Intermetallic Alloys V; Mater. Res. Soc. Symp. Proc.* **288**
[2] Darolia R, Lewandowski J J, Lui C T, Martin P L, Miracle D B and Nathal M V 1993 *Structural Intermetallics* (Warrendale, PA: Metallurgical Society of the AIME)
[3] Stoloff N S and Liu C T 1996 *Physical Metallurgy and Processing of Intermetallic Compounds* ed N S Stoloff and V K Sikka (New York: Chapman & Hall) p 159
[4] Lui C T and Horton J A 1995 *Mater. Sci. Eng.* A **192+193** 170
[5] Smiallek J L 1978 *Metall. Trans.* A **9** 309
[6] Anton D L, Shah D M, Duhl D N and Giamei A F 1989 *J. Met.* **41** 12
[7] Smith M E 1993 *Appl. Magn. Reson.* **4** 1

[8] Knight W D 1949 *Phys. Rev.* **76** 1259
[9] Drain L E 1967 *Metall. Rev.* **119** 195
[10] Carter G C, Bennett L H and Kahan D J 1977 *Metallic Shifts in NMR* (Oxford: Pergamon)
[11] Bastow T J and Smith M E 1995 *J. Phys.: Condens. Matter* **7** 4929
[12] West G W 1964 *Phil. Mag.* **9** 979
[13] Miyatani K and Iida S 1968 *J. Phys. Soc. Japan* **25** 1008
[14] Brettell J M and Hinshaw W S 1976 *J. Phys. F: Met. Phys.* **6** 1177
[15] Crousier J, Crousier J-P, Streiff R and Vincent E-J 1977 *Acta Metall.* **25** 619
[16] Rubini S, Dimitropoulos C, Aldrovandi S, Borsa F, Torgeson D R and Ziolo J 1992 *Phys. Rev.* B **46** 10 563
[17] Rubini S, Dimitropoulos C and Borsa F 1994 *Phys. Rev.* B **49** 9331
[18] Golberg D and Shevakin A 1994 *Intermetallics* **2** 147
[19] Smith M E, Gibson M A, Forwood C T and Bastow T J 1996 *Phil. Mag.* A **74** 791
[20] Cohen M H and Rief F 1957 *Solid State Physics* vol 5 (New York: Academic) p 321
[21] Bradley A J and Taylor A 1937 *Phil. Mag.* **23** 1049
[22] Kunwar A C, Turner G L and Oldfield E 1986 *J. Magn. Reson.* **69** 124
[23] *CRC Handbook of Chemistry and Physics* 1996 ed D R Lide (Boca Raton, FL: Chemical Rubber Company Press) pp 9–85
[24] Hackenbracht D and Kuebler J 1980 *J. Phys. E: Sci. Instrum.* **10** 427
[25] Seymour E F W 1957 *Proc. Phys. Soc.* A **A66** 85
[26] Drain L E and West G W 1965 *Phil. Mag.* **11** 1061
[27] Baugher J F, Taylor P C, Oja T and Bray P J 1969 *J. Chem. Phys.* **50** 4914